Silencing Herg1 by shRNA inhibits the proliferation and invasion of osteosarcoma in vivo and in vitro

Zhida Chen
Affiliated Dongnan Hospital of Xiamen University
Chao Song
Affiliated Dongnan Hospital of Xiamen University
Yunping Chen
910th Hospital of PLA
Lili Xiao
Affiliated Dongnan Hospital of Xiamen University
Yuanjie Jiang
Affiliated Dongnan Hospital of Xiamen University
Jin Wu (wujin1983@xmu.edu.cn)
Affiliated Dongnan Hospital of Xiamen University https://orcid.org/0000-0002-6041-4462

Research article

Keywords: Herg1, Osteosarcoma, Hippo signaling pathway, YAP, Tumorigenicity

DOI: https://doi.org/10.21203/rs.3.rs-331716/v1

Abstract

Background: Osteosarcoma is the most common malignant bone tumor of childhood, and improvements in the survival rates have reached a plateau phase. This study was aimed to explore the the importance of the human ether-a-go-go-related potassium channel (Herg1) in the proliferation and invasion of osteosarcoma.

Methods: The effects of Herg1 silenced on osteosarcoma cell proliferation and invasion were detected by were detected by CCK-8 assay, wound healing assay and transwell assay, respectively. Tandem affinity purification, mass spectrometry and Dual luciferase reporter assay were used to find out possible molecules responsible for the action of Herg1 on osteosarcoma cells. Nude mouse model was used to investigate the *in vivo* functions of Herg1.

Results: Herg1 silencing by shRNA significantly suppressed the proliferation and invasion of osteosarcoma cells *in vitro* as well as tumorigenicity and metastasis in nude mice. Moreover, Herg1 promoted osteosarcoma progression via turning off Hippo signaling pathway, leading to the activation of Yes-associated protein (YAP). Mechanistically, Herg1 co-localized and interacted with *NF2* (also called Merlin), and this interaction probably caused the de-phosphorylation of MST1/2 and LATS1/2, which drove YAP nuclear translocation and transcriptional activation.

Conclusion: Herg1 acts as an oncogene in osteosarcoma and may therefore serve as a useful therapeutic target for osteosarcoma patients.

Introduction

Osteosarcoma, arising from the malignant osteoblasts, is the most common malignant bone tumor in children and adolescence [1, 2]. Current treatments for osteosarcoma by combining surgery with neoadjuvant chemotherapy, metastatic or recurrent osteosarcomas survival rates have changed little in the past 30 years, 5-year survival rates of patients presenting metastatic disease have only reached 20%. However, there are about 40–50% of patients will develop metastases [3]. Thus, it is extremely vital to further understand the mechanism of tumorigenesis in osteosarcoma and the need to find new therapeutic targets is urgent.

Accumulating evidence suggests that Hippo signaling (also known as the Salvador/Warts/Hippo pathway) is involved in cancer development including osteosarcoma [4–8]. The canonical Hippo signaling cascade involves several essential components: MST1/2 (mammalian sterile 20-like kinases 1/2), SAV1 (salvador family WW domain-containing protein 1), LATS1/2 (large tumor suppressor kinases 1/2) and YAP. As a serine/threonine kinase, MST1/2 forms complex with Sav1 to phosphorylate and activate LATS1/2, whose activation in turn phosphorylates YAP at Ser127 and enhances its degradation [9, 10]. On the contrary, inactivation of MST1/2 and LAST1/2 releases YAP phosphorylation and promotes its nuclear translocation, where dephosphorylated YAP acts as a transcriptional coactivator to regulate gene expression via interacting with multiple transcription factors. Although the significance of

the Hippo signaling pathway has been documented in osteosarcoma, the upstream molecules responsible for its regulation are largely unknown.

NF2, also called Merlin, is associated with neurofibromatosis type 2 (NF2) [11, 12]. Recent studies also demonstrated that *NF2* mutation or inactivation was observed in multiple cancers [13–16], suggesting its significance in cancer progression. The functional loss of *NF2* could trigger numerous signaling pathways including MAPK, AKT and Hippo [13]. Particularly, *NF2* represents one of the regulatory molecules involved in the Hippo signaling cascade as a tumor suppressor.

Recently, the functional role of voltage-gated potassium (Kv) channels in cancer biology has been an investigative highlight area. Several Kv channels, especially Herg1 (Kv11.1, KCNH2) channel, have shown an intimate relationship to cancer growth, progression and metastasis [17–20]. Although our previous study preliminarily demonstrated overexpression of Herg1 in osteosarcoma [21], the detailed mechanical action of Herg1 in osteosarcoma initiation and progression, especially invasion and metastasis, is still poorly understood.

In this study, we identified that Herg1 co-localized and interacted with *NF2*, which led to the phosphorylation of MST1/2 and LAST1/2. For this reason, YAP was activated and exerted its role as a transcriptional cofactor to regulate gene expression. Attenuation of Herg1 expression could suppress the cell proliferation and cell invasion of osteosarcoma cells *in vitro*. Furthermore, reduction of Herg1 bore the ability to suppress the xenografted tumor growth and to inhibit tumor metastasis in the tail vein injection mouse model. Overall, all these data build a rationale to develop Herg1 as a diagnosis and target for osteosarcoma patients in therapies.

Materials And Methods

Cell culture

Human osteosarcoma cell lines U2OS and 143B, and human embryonic kidney 293T cells (HEK293T) were obtained from the Institute of Biochemistry and Cell Biology, Chinese Academy of Sciences, Shanghai. U2OS cells were maintained in RPMI 1640 medium (Gibco, Rockville, MD, USA) supplemented with 10% fetal bovine serum (Gibco). HEK293T and 143B cells were cultured in DMEM medium (Gibco) supplemented with 10% fetal bovine serum (Gibco). All cell lines were maintained at 37ºC, in a humidified atmosphere in 5% CO_2.

Quantitative PCR

RNAs isolated from osteosarcoma cells were subjected to reverse transcription by Trizol reagent (Invitrogen, Rockville, MD, USA). qPCR was carried out using a Bio-Rad CFX96 system (Bio-Rad, Richmond, CA, USA) with SYBR green (Invitrogen) to determine the mRNA expression level of interest genes. Each sample contained 0.5 μL cDNA, 7.5 μL DEPC water, 10.0 μL SYBR green, and 2.0 μL gene primers in a total volume of 20 μL and was run in duplicate according to the following protocol: DNA denaturation at 94 °C for 4 min, followed by 30 amplification cycles consisting of 45 s at 94 °C, 45 s at

54 ℃, and 45 s at 72 ℃. Expression levels were normalized to the GAPDH level. The following primers were applied in qPCR:

Herg1, forward, 5’-GGA CGC GCT CCC GAG AAA – 3’;

Herg1, reverse, 5’- GCT GCG CAG TGG GTG CAT – 3’;

CTGF, forward, 5’-AAT GCT GCG AGG AGT GGG TGT – 3’;

CTGF, reverse, 5’-TGG ACC AGG CAG TTG GCT CTA – 3’.

BIRC5, forward, 5’-AGG ACC ACC GCA TCT CTA CAT – 3’;

BIRC5, reverse, 5’-AAG TCT GGC TCG TTC TCA GTG – 3’.

ANKRD1, forward, 5’-CGT GGA GGA AAC CTG GAT GTT – 3’;

ANKRD1, reverse, 5’-GTG CTG AGC AAC TTA TCT CGG – 3’.

CYR61, forward, 5’-TGC GGC TGC TGT AAG GTC TG -3’;

CYR61, reverse, 5’-TCT GCC CTC TGA CTG AGC TCT G -3’.

18S, forward, 5’-CGA CGA CCC ATT CGA ACG TCT – 3’;

18S, reverse, 5’-CTC TCC GGA ATC GAA CCC TGA – 3’.

Each experiment was performed at least three times with representative data presented.

Herg1 knockdown

The lentivirus-based vector pLKO.1 was used for the expression of shRNA in osteosarcoma cells. ShRNAs were co-transfected with the packaging plasmids (psPAX2 and pMD2G) in 293T cells using the standard calcium phosphate transfection method. 48 h post-transfection, supernatants were collected and infected cells for 24 h in the presence of polybrene (8μg/ml). After infection, puromycin (1.0 μg/ml) was used to select stably transduced cells. The targeting sequences for human Herg1 were 5'- CTC ACC TTG GAC TCG CTT TCT-3' (Sh1-Herg1), 5'-CAG ATA GGC AAA CCC TAC AAC-3' (Sh2-Herg1). The non-targeting sequence 5'- TTC TCC GAA CGT GTC ACG T-3' was used as control (shCtr).

Cell proliferation assay

For cell proliferation assay, osteosarcoma cells transfected with shCtr, shHerg1, or shHerg2 in serum-free medium were seeded on 96-well plates (Sigma, St. Louis, MO, USA) with a density of 3×10^3 cells/100 μl for 12 h. After incubation for 96 h, the cells were stained with 10 μl CCK8 reagent (Cat: QF0025, Qiancheng Biotech, Shanghai) at each time point for 1 h at 37°C. The absorbance value was determined using spectrophotometer (Bio-Rad) at 450 nm wavelength. All experiments were replicated in triplicates.

Wound healing assay

Osteosarcoma cells stable transfected with shCtr or shHerg1 were seeded into a 6-well plate (Sigma) at a density of 5×10^5 cells/well. The wound was generated using a 10 ìL plastic pipette tip with a straight scratch when cells confluence reached 80%. Cells were continued to culture for 24 h in the serum-free medium after three times wash in PBS. Finally, the wound was observed under an inverted microscope.

Transwell assay

Migration and invasion assays were performed using Transwell plates (Corning, NY, USA) with 8 ìm-pore size membranes without Matrigel (for migration assays) or with 50 µl Matrigel (for invasion assays). 2×10^5 cells/well of osteosarcoma with or without manipulation of Herg1 expression were added to each Transwell upper chamber. After 24 h incubation at 37ºC, migrated cells were fixed with 4% formaldehyde and stained with 0.5% toluidine blue. And then counted from six random fields. For invasion assay, the membrane of the upper chambers was precoated with 5 folds diluted matrigel (BD Biosciences, Sparks, MD) before use. Migrating or invading osteosarcoma cells were counted and photographed under high view of microscope (200×).

Tandem affinity purification and mass spectrometry

pLV-tagII-Herg1 or pLV-tagII-GFP control stable transfected 143B cells were seeded in 75 cm^2 dishes with 2×10^6 cells per dish (20 dishes per condition). Cell pellets were lysed in TBST Buffer (Sigma). Protein extract was incubated overnight with Streptactin affinity beads (GE Healthcare) at 4°C. Then protein complexes were eluted with Desthiobiotin elution buffer having 30 mM Tris-HCl, 150 mM NaCl, 2 mM desthiobiotin and incubated with Flag M2 beads for 2 h in TBST Buffer. Proteins were finally eluted with 3 × Flag peptide and heated at 95°C for 10 min. Western blot analysis was conducted for the eluted proteins after centrifugation.

200 µl protein eluent was taken, 700 µl pre-cooled acetone was added, the solutions were thoroughly mixed and stored at -20 ℃ for 4 h. They was centrifuged at 16,000 r/min for 20 min at 4°C and then washed with pre-cooled acetone for 2 times. Protein was resuspended in 10 µl of double-distilled water, 2.5 µl protein loading buffer was added, boiled for 10 min and gel electrophoresis was performed by 12% sodium dodecyl sulfate-polyacrylamide gel electrophoresis (SDS-PAGE). After the gel was stained with protein silver staining kit, the differential bands were extracted from the gel and digested with trypsin. The obtained peptides were analyzed and identified by AB Sciex Triple TOF 5600 system (Framingham, MA, US).

The proteins that interacted with Herg1 identified by mass spectrometry, as well as bovine serum albumin (BSA) and glutathione-S-transferase (GST) as negative controls were gradient-diluted. The final concentration of each protein was 8, 2, 0.5 and 0 µmol/L, respectively. The samples were then loaded onto nitrocellulose membrane from left to right and sealed with solution F (25 mmol/L Tris HCl, 150 mmol/L NaCl, 5% skimmed milk powder, 1 mmol/L EDTA) for 2 h at room temperature. MutM-SBP was added into culture medium with the final concentration of 16 µmol/L and incubated for 1h. The membranes were washed with solution E (25 mmol / L Tris HCl, 150 mmol / L NaCl, 0.05% Tween-20) and solution E without Tween-20 for 3 times, respectively. After washing, streptavidin-alkaline

phosphatase diluted 1:3000 were added and incubated for 1 h at room temperature. The washes were repeated 3 times. Then were stained using nitroblue tetrazolium/5-bromo-4-chloro-3-indolyl phosphate (NBT/BCIP) at 37 ºC and take photos.

Dual luciferase reporter assay

HEK293T cells in the logarithmic growth phase were seeded into a 24-well plate (Sigma) at a density of 2 × 10^5 cells/mL. And then seeded at 100 μl per well in a 24-well plate and cultured for 24 h. Next, cells were washed gently 3 times with PBS and co-transfected with pLV-Herg1/control (200 ng/well) and CTGF- luciferase plasmids (200 ng/well). The cells were lysed at 48 h post-transfection, and the luciferase activity was measured using the Glomax 20/20 luminometer (Promega).

Immunofluorescence staining

HEK293T cells seeded on the sterile coverslip in six-well plates were incubated for 48 h. Afterward, cells were fixed with 4% paraformaldehyde for 20 min, followed by rinsed third with PBS. The fixed cells were permeabilized with 0.1% Triton X-100-PBS for 10 min at room temperature, washed three with PBS and blocked with 2% bovine serum albumin (BSA) for 30 min. And then incubated with mouse anti-Flag (Cat: YM1222, Immunoway Biotech, Plano, TX, USA) and rabbit anti-HA antibodies (Cat: YG0003, Immunoway Biotech) in blocking solution. After incubation at 37ºC for 1 h and being rinsed four times (5 min each) with washing buffer, wells were probed with secondary antibody conjugated with Alexa Fluorescence 488, 594, or 633 (Invitrogen) in blocking solution in the dark at 37°C for 1 h. Finally, the cell nuclei were counterstained with DAPI (1 μg/ml) in washing solution for 10 min, washed four times with washing buffer. The coverslips were then mounted with glycerol and sealed with nail polish. Images were captured using a laser confocal microscope (Zeiss).

Western Blotting

5–6×10^7 cells were collected and the cells were lysed by 4 ℃ precooled lysate for 30 min. The lysates were centrifuged at 13,200 rpm for 10 min at 4 ℃. The supernatants were collected and determined the protein concentration by BCA protein assay kit (Qiancheng Biotech, Shanghai). 20 μg protein were resolved by a 12% SDS-PAGE and blotted on nitrocellulose membranes (Bio-Rad). Membranes were blocked with 10% (w/v) skim milk powder for 1 h at room temperature, and then incubated with antibodies against Herg1 (Cat: D160470, Sangon Biotech), YAP (Cat:13584-1-AP, Proteintech Biotech, Rosemont, IL, USA), p-YAP (Ser123) (Cat: D151452, Sangon Biotech), LATS1 (Cat: 17049-1-AP, Proteintech Biotech), p-LATS1 (Thr1079/1041) (Cat: YP1222, Immunoway Biotech), anti-Flag (Cat: YM1222, Immunoway Biotech), anti-HA (Cat: YG0003, Immunoway Biotech) and GAPDH (Cat: 60004-1-AP, Proteintech Biotech) at 4 ℃ overnight, followed by incubation with horseradish corresponding secondary antibody (Sangon Biotech). Then the membranes were developed with ECL chemiluminescent detection kit (Sangon Biotech) and exposed to X-ray films. The relative expression level of target protein = gray value of target protein / gray value of GAPDH. All the experiments were performed at least three times with similar results and representative data.

Animal studies

All animal experiments were performed according to guidelines approved by the Animal Care and Use Committee of Xiamen University.
All animal experiments were performed according to guidelines approved by the Animal Care and Use Committee of Xiamen University.
Animal studies were performed at the animal center of Xiamen University. All animal experiments were performed according to guidelines approved by the Animal Care and Use Committee of Xiamen University. Nude mice were supplied by the Xiamen laboratory animal center. Firstly, We established a xenograft model of osteosarcoma in nude mice. 1×10^6 cells 143B cells infected with or without lentivirus particles were subcutaneously injected into the lower back regions of 6-week-old male nude mice (n = 6 per group). After the inoculation, the tumor length (L) and width (W) were measured weekly. Tumor volume = $1/2 \times L \times W^2$. After 5 weeks, the mice were sacrificed and the weight of transplanted tumor was weighed. For the Metastasis cancer model, 2×10^6 luciferase expressing 143B cells with or without shHerg1 were injected into the tail veins of nude mice for 5 weeks (n = 6 per group). Tumor growth at day 35 was dynamically monitored using the In Vivo Imaging System (IVIS). And the fluorescence signal was collected for 1 min.

Statistical analysis

All statistical analyses were with SPSS 19.0. The data values were presented as the mean ± Standard Error of Mean (SEM). Between two groups, comparisons in mean values were analyzed by independent Student's t test. *P*-value < 0.05 represents differences statistically significant between means.

Results

Knockdown of Herg1 suppressed the proliferation and invasion of osteosarcoma cells

To delineate the role of Herg1 in the osteosarcoma carcinogenesis, we reduced Herg1 expression by two independent shRNAs whose efficiencies were confirmed (Fig. 1a protein level, Left and mRNA level, Right). We detected the effects of Herg1 knockdown on the proliferation and invasion of osteosarcoma cells. Attenuation of Herg1 expression led to a dramatic suppression of cell proliferation of 143B cellsin (Fig. 1b). Furthermore, reduction of Herg1 also decreased the cell migration, which was monitored by wound healing assay (Fig. 1c) and non-matrigel transwell assay (Fig. 1d), as well as cell invasion examined by matrigel transwell assay (Fig. 1e). To confirm the phenotypic contribution of Herg1 to cell proliferation and invasion of 143B cells is not cell-context dependent, we performed the same assays in another osteosarcoma cell line, U2OS.

After efficient reduction of Herg1 in U2OS cells (Fig. 2a), the proliferating rate and migrating/invasive ability of U2OS cells were investigated. Consistent with previous results, shHerg1 significantly suppressed cell growth (Fig. 2b) and reduced cell migration/invasion (Fig. 2c-e) in U2OS cells, supporting the notion that the Herg1 functions as an oncogenic factor in osteosarcoma cells.

Herg1 formed complex with NF2

To find which molecules responsible for the action of Herg1 on osteosarcoma cells, we performed tandem affinity purification to pull down Herg1 and its associated complex. With the identification of Herg1 on this purification by silver staining (Fig. 3a) and western blotting (Fig. 3b), we subjected these elutes to do Mass Spectrum analysis. Intriguingly, *NF2* was characterized as a component of Herg1-purified complex, suggesting *NF2* may interact with Herg1. To further confirm the physical binding between NF2 and Herg1, immunoprecipitation assay were performed by using the Flag-Herg1 and HA-*NF2* transfected 293T cells. HA-*NF2* could be detected in anti-Flag elutes, indicating *NF2* associated with Herg1 (Fig. 3c). Similarly, HA-*NF2* was co-localized with Flag-Herg1 in the cell membrane of 293T cells monitored by immunofluorescent staining assay (Fig. 3d). Together, these data indicate that *NF2* interacts with Herg1 in the cell membrane.

Deficiency of Herg1 turned on Hippo signaling pathway

Given the fact that *NF2* acts as an upstream molecule to turn on the Hippo cascade and *NF2* interacts with Herg1, we sought to investigate whether Herg1 could affect the Hippo signaling pathway. To end this, we simply tested whether altered Herg1 had the capacity to influence CTGF luciferase activity, which is used to reflect the transcriptional activity of Hippo pathway effector YAP. Surprisingly, knockdown of Herg1 had the ability to decrease the CTGF luciferase activity in both 143B cells (Fig. 4a) and U2OS cells (Fig. 4b), proving that Herg1 could promote the transcriptional activity of YAP. To further confirm this, we detected several YAP targeting gene expressions (CTGF, BIRC5, CYR61 and ANRKD1) after the manipulation of Herg1 in osteosarcoma cells. The results revealed that these YAP targeting genes were obviously silenced when Herg1 was knocked down (Fig. 4c-d). Consistently, the levels of LAST1/2 and YAP phosphorylation were evidently elevated in Herg1-deficient 143B cells (Fig. 4e) and U2OS cells (Fig. 4f). Collectively, these results imply that Herg1 could enhance the transcriptional activity of YAP by turning off Hippo signaling, which is probably mediated by interacting with *NF2.*

Deficiency of Herg1 suppressed tumor growth and tumor metastasis *in vivo*

The convincing *in vitro* evidence prompted us to investigate the *in vivo* functions of Herg1 in a nude mouse model. We first established *in vivo* mouse models *via* subcutaneously xenografting 1×10^6 143B cells with or without Herg1 into nude mice (n = 6 for each group). After the inoculation, the tumor weight was measured weekly and the mice were sacrificed 5 weeks later. The results showed that tumor growing rate was considerably lower in shHerg1 bearing mice (Fig. 5a and b)compared to the control cohorts. Consistent with our *in vitro* findings, the levels of LAST1/2 and YAP phosphorylation were also elevated in tumors derived from shHerg1 deficient mice (Fig. 5c). These data suggest that knockdown of Herg1 could suppress the tumor growth of osteosarcoma. In tail-vein metastasis mouse model, 2×10^6 luciferase expressing 143B cells were injected into mice by tail veins. 5 weeks later, a dramatic decrease of metastatic luciferase signal was found in the shHerg1 group compared to the control group by the IVIS (Fig. 5d), proving that knockdown of Herg1 could reduce the metastasis of osteosarcoma. Taken together, the results from *in vivo* mouse model studies are consistent with the above *in vitro* cell lines studies. They imply that targeting Herg1 could inhibit the growth and metastasis of osteosarcoma *via* regulation of the Hippo signaling pathway.

Discussion

The incidence rate of osteosarcoma is the highest in children and adolescents' malignant bone tumors and has a tendency of local invasion and early lung metastasis [1]. The mainstay treatments for osteosarcoma include surgery, chemotherapy and radiation. However, the 10-year disease-free survival rate of patients with localized disease is about 60%, and the patients with metastases at diagnosis confer a poor prognosis [21]. So the treatment of osteosarcoma is far from satisfactory. It is a desired need to identify novel therapeutic targets and to develop target-based therapeutic strategies.

Recently, growing evidence indicates that Herg1 is aberrantly expressed in different human tumor cells and negatively expressed in non-cancerous matched tissues. Moreover, Herg1 is involved in the proliferation, apoptosis, invasion and some other malignant phenotype of tumor [22]. Nevertheless, studies investigating the role of Herg1 in human osteosarcoma are rare. Indeed, it was recently suggested that Herg1 is overexpressed in osteosarcoma and its expression might affect the osteosarcoma cell proliferation and apoptosis [20]. In addition, the regulatory mechanisms of Herg1 expression in osteosarcoma invasion and metastasis are still unclear.

Hippo signaling has been documented as crucial player in the development of chemo-resistance [7]. For osteosarcoma patients, the use of methotrexate and doxorubicin in clinical are common. However, drug resistance will invariably occur and hamper their further implications. Wang et al. demonstrated that MG63 cells expressing YAP were more resistant to methotrexate or doxorubicin treatment, while susceptibility to methotrexate or doxorubicin treatment was observed in YAP deficient MG63 cells [7], implying YAP is required and sufficient to cause chemo-resistance in osteosarcoma cells. Herein, we first showed that Herg1 knockdown could silence the transcriptional activity of YAP. Therefore, we believe Herg1 may also be a causal factor for the development of chemo-resistance in osteosarcoma cells. It is worth testing whether targeting Herg1 could alleviate chemo-resistance and increase the anti-cancer efficacy of methotrexate or doxorubicin.

As a tumor suppressor, *NF2* interacts and retains YAP in the cell membrane, blocking its nuclear trafficking [11]. *NF2* loss or mutation could activate the Hippo signaling pathway by releasing YAP from the cell membrane. Here, our results suggested that Herg1 could interact and co-localize with *NF2* in the cell membrane. It is possible that Herg1 compete with YAP for the interaction of *NF2.* In osteosarcoma cells, the overexpressed Herg1 overrides YAP to bind *NF2*, resulting in the nuclear entry of YAP and eliciting YAP dependent transcription. Moreover, our study also showed that the phosphorylation levels of LAST1/2 were increased after knockdown of Herg1, suggesting Herg1 could also regulate YAP activation independent of *NF2* presence.

Our previous study found that knockdown of Herg1 could suppress proliferation and invasion of osteosarcoma cells by negatively regulating NF-κB targeting genes such as cIAP-1, Bcl2, MMP2 and MMP9 [20]. Our further data revealed that the loss of Herg1 also suppressed YAP activity. As a transcription cofactor, we hypothesize that YAP has the capacity to cooperate with NF-κB to regulate its targeting genes. Therefore, the regulation on NF-κB targeting genes by Herg1 may rely on Hippo/YAP

signaling pathway. A relevant question to approach in further experiments is to investigate this crosstalk in Herg1 overexpressed osteosarcoma cells and this will be our next aim.

In this study, knockdowning Herg1 reveals inhibition of cell proliferation and cell invasion/migration of osteosarcoma cells by turning on the Hippo signaling pathway and shutting down YAP activation. Mechanistic dissection revealed that Herg1 interacts and co-localizes with *NF2* in the cell membrane, which relieves its inhibitory effect on YAP. Importantly, our findings were also validated in mouse model showing that attenuation of Herg1 suppressed tumor growth and tumor metastasis.

Conclusion

In conclusion, our data provide evidence that Herg1 could positively regulate YAP activation, leading to osteosarcoma progression *in vitro and in vivo* and targeting Herg1 might afford a new therapeutic strategy for osteosarcoma.

Abbreviations

Herg1: Human ether-a-go-go-related potassium channel; HEK293T: Human embryonic kidney 293T cells; Kv: Voltage-gated potassium; LATS1/2: Large tumor suppressor kinases 1/2; MST1/2: Mammalian sterile 20-like kinases 1/2; NF2: Neurofibromatosis type 2; SAV1: Salvador family WW domain-containing protein 1; YAP: Yes-associated protein.

Declarations

Acknowledgements

Not applicable.

Authors' Contributions

Jin Wu designed the study. Zhida Chen and Chao Song contributed to the literature research, experimental studies and manuscript editing. Yunping Chen undertook the data collection. Lili Xiao and Yuanjie Jiang analyzed the data. All authors read and approved the final manuscript.

Funding

This study was supported by The Natural Science Foundation of China (Nos. 81402217) and The Natural Science Foundation of Zhangzhou (ZZ2018J10).

Availability of data and materials

Request for details in the study dataset can be submitted to the corresponding author.

Ethics approval and consent to participate

The animal study protocol has been reviewed and approved by the Animal Ethics Committee of the Affiliated Southeast Hospital of Xiamen University (No. P2018-017-3).

Consent for publication

Not applicable.

Competing interests

The authors declared that they have no conflict of interest.

Author details

[1]Department of Orthopaedics, the Affiliated Southeast Hospital of Xiamen University, Orthopaedic Center of People's Liberation Army, Fujian Province, Zhangzhou 363000, China.

[2]Department of Oncology, the 910th Hospital of People's Liberation Army, Fujian Province, Quanzhou 362000, China.

[3]Department of Ultrasound, the Affiliated Southeast Hospital of Xiamen University, the 909th Hospital of People's Liberation Army, Fujian Province, Zhangzhou 363000, China.\

References

1. Sluga M, Windhager R, Pfeiffer M, Ofner P, Lang S, Dominkus M, Nehrer S, Zoubek A, Kotz R. Osteosarcoma and ewing's sarcoma--the most frequent malignant bone tumors in children--therapy and outcome. Z Orthop Ihre Grenzgeb. 2002;140:652-655.
2. Damron TA, Ward WG, Stewart A. Osteosarcoma, chondrosarcoma, and ewing's sarcoma: national cancer data base report. Clin Orthop Relat Res. 2007;459:40-47.
3. Rosen G, Caparros B, Huvos AG, Kosloff C, Nirenberg A, Cacavio A, Marcove RC, Lane JM, Mehta B, Urban C. Preoperative chemotherapy for osteogenic sarcoma: selection of postoperative adjuvant chemotherapy based on the response of the primary tumor to preoperative chemotherapy. Cancer. 1982;49:1221-1230.
4. Harvey K, Tapon N. The Salvador-Warts-Hippo pathway-an emerging tumour-suppressor network. Nat Rev Cancer. 2007;7:182-191.
5. Cordenonsi M, Zanconato F, Azzolin L, Forcato M, Rosato A, Frasson C, Inui M, Montagner M, Parenti AR, Poletti A, Daidone MG, Dupont S, Basso G, Bicciato S, Piccolo S. The Hippo transducer TAZ confers cancer stem cell-related traits on breast cancer cells. Cell. 2011;147:759-772.
6. Zhang X, George J, Deb S, Degoutin JL, Takano EA, Fox SB; AOCS Study group, Bowtell DD, Harvey KF. The Hippo pathway transcriptional co-activator, YAP, is an ovarian cancer oncogene. Oncogene. 2011;30:2810-2822.

7. Wang DY, Wu YN, Huang JQ, Wang W, Xu M, Jia JP, Han G, Mao BB, Bi WZ. Hippo/YAP signaling pathway is involved in osteosarcoma chemoresistance. Chin J Cancer. 2016;35:47.
8. Ma J, Huang K, Ma Y, Zhou M, Fan S. The TAZ-miR-224-SMAD4 axis promotes tumorigenesis in osteosarcoma. Cell Death Dis. 2017;8:e2539.
9. Wu S, Huang J, Dong J, Pan D. Hippo encodes a Ste-20 family protein kinase that restricts cell proliferation and promotes apoptosis in conjunction with salvador and warts. Cell. 2003;114:445-456.
10. Chan EH, Nousiainen M, Chalamalasetty RB, Schäfer A, Nigg EA, Silljé HH. The Ste20-like kinase Mst2 activates the human large tumor suppressor kinase Lats1. Oncogene. 2005;24:2076-2086.
11. Lavado A, He Y, Paré J, Neale G, Olson EN, Giovannini M, Cao X. Tumor suppressor Nf2 limits expansion of the neural progenitor pool by inhibiting Yap/Taz transcriptional coactivators. Development. 2013;140:3323-3334.
12. Striedinger K, VandenBerg SR, Baia GS, McDermott MW, Gutmann DH, Lal A. The neurofibromatosis 2 tumor suppressor gene product, merlin, regulates human meningioma cell growth by signaling through YAP. Neoplasia. 2008;10:1204-1212.
13. Garcia-Rendueles ME, Ricarte-Filho JC, Untch BR, Landa I, Knauf JA, Voza F, Smith VE, Ganly I, Taylor BS, Persaud Y, Oler G, Fang Y, Jhanwar SC, Viale A, Heguy A, Huberman KH, Giancotti F, Ghossein R, Fagin JA. NF2 loss promotes oncogenic RAS-induced thyroid cancers via YAP-dependent transactivation of RAS proteins and sensitizes them to MEK inhibition. Cancer Discov. 2015;5:1178-1193.
14. Murray LB, Lau YK, Yu Q. Merlin is a negative regulator of human melanoma growth. PLoS One. 2012;7:e43295.
15. Bianchi AB, Hara T, Ramesh V, Gao J, Klein-Szanto AJ, Morin F, Menon AG, Trofatter JA, Gusella JF, Seizinger BR, Kley N. Mutations in transcript isoforms of the neurofibromatosis 2 gene in multiple human tumour types. Nat Genet. 1994;6:185-192.
16. Yoo NJ, Park SW, Lee SH. Mutational analysis of tumour suppressor gene NF2 in common solid cancers and acute leukaemias. Pathology. 2012;44:29-32.
17. Afrasiabi E, Hietamäki M, Viitanen T, Sukumaran P, Bergelin N, Törnquist K. Expression and significance of Herg (KCNH2) potassium channels in the regulation of MDA-MB-435S melanoma cell proliferation and migration. Cell Signal. 2010;22:57-64.
18. Glassmeier G, Hempel K, Wulfsen I, Bauer CK, Schumacher U, Schwarz JR. Inhibition of Herg1 K^+ channel protein expression decreases cell proliferation of human small cell lung cancer cells. Pflugers Arch. 2012;463:365-376.
19. Lastraioli E, Guasti L, Crociani O, Polvani S, Hofmann G, Witchel H, Bencini L, Calistri M, Messerini L, Scatizzi M, Moretti R, Wanke E, Olivotto M, Mugnai G, Arcangeli A. Herg1 gene and Herg1 protein are overexpressed in colorectal cancers and regulate cell invasion of tumor cells. Cancer Res. 2004;64:606-611.

20. Zeng W, Liu Q, Chen Z, Wu X, Zhong Y, Wu J. Silencing of Herg1 gene inhibits proliferation and invasion, and induces apoptosis in human osteosarcoma cells by targeting the NF-kappaB pathway. J Cancer. 2016;7:746-757.
21. Longhi A, Errani C, De Paolis M, Mercuri M, Bacci G. Primary bone osteosarcoma in the pediatric age: State of the art. Cancer Treat Rev. 2006;32:423-436.
22. Lastraioli E, Lottini T, Bencini L, Bernini M, Arcangeli A. Herg1 potassium channels: novel biomarkers in human solid cancers. Biomed Res Int. 2015;2015:896432.

Figures

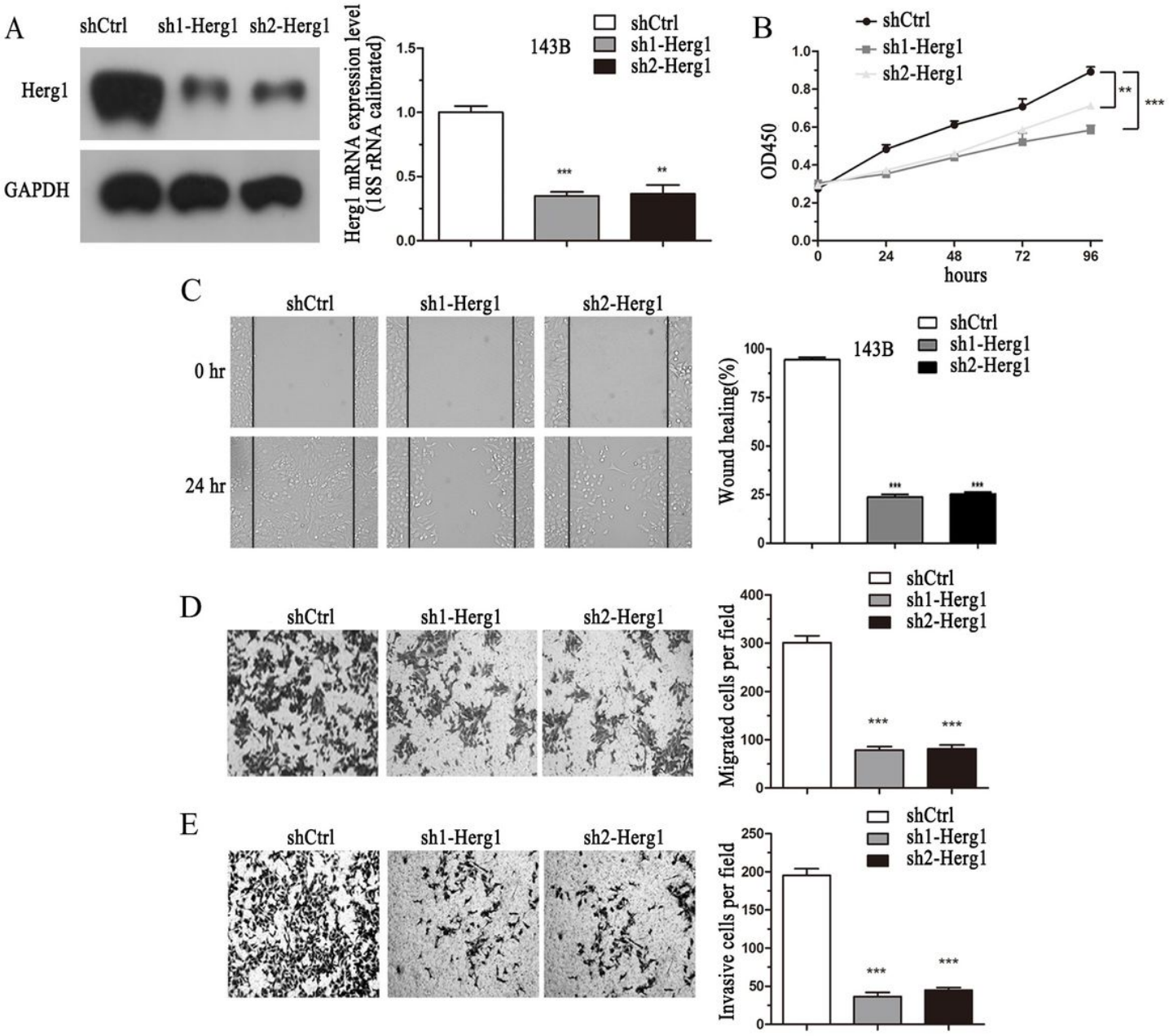

Figure 1

Knockdown of Herg1 suppressed cell growth and cell invasion of 143B cells. a The efficiency of knocking down Herg1 in 143B cells was examined by western blotting (Left) and qPCR (Right). GAPDH was served as loading control for western blotting, mRNA levels of Herg1 was normalized to ribosomal 18s RNA. b Deficiency of Herg1 suppressed the proliferating rate of 143B cells. c Wound healing assay showed that shHerg1 reduced cell migration in 143B cells. d Non-matrigel transwell assay confirmed that the cell migrating ability of Herg1 deficient 143B cells was decreased. Representative images were displayed (Left) and statistical analysis was made (Right). e Results from matrigel transwell assay showed that the invasive ability of Herg1 deficient 143B cells was decreased. Representative images were displayed (Left) and statistical analysis was made (Right). **P < 0.01, ***P < 0.001.

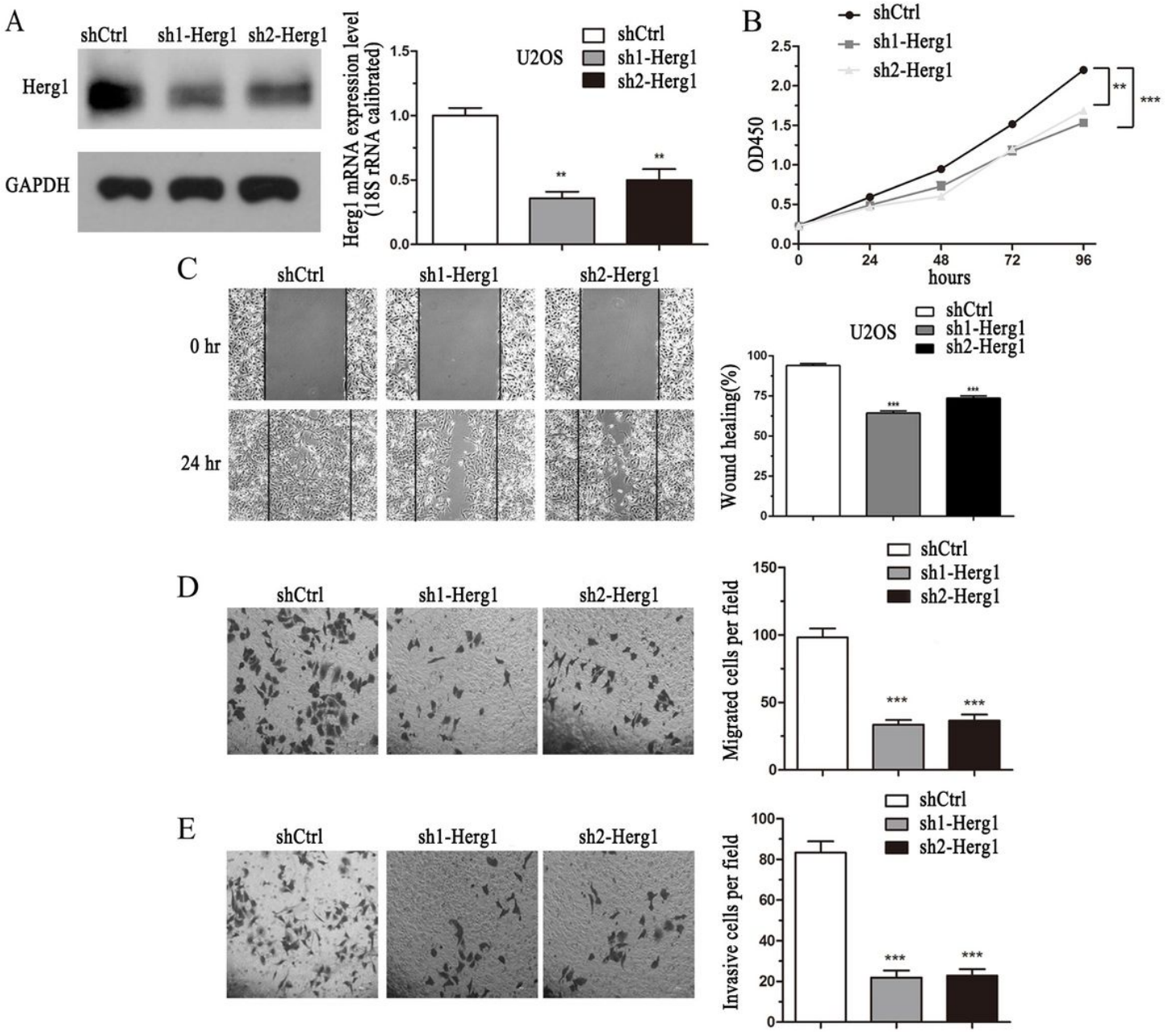

Figure 2

Attenuation of Herg1 inhibited cell proliferation and cell invasion of U2OS cells. a Knocking down efficiency of Herg1 in U2OS cells was examined by western blotting (Left) and qPCR (Right). GAPDH was served as loading control for western blotting, mRNA levels of Herg1 was normalized to ribosomal 18s RNA. b Reduction of Herg1 by shRNA inhibited the proliferating rate of U2OS cells. c The migrating ability of U2OS cells was decreased when Herg1 levels was silenced, which was monitored by wound healing assay. d Cell migration of U2OS cells were reduced after Herg1 knockdown, which was monitored by non-matrigel transwell assay. Representative images were displayed (Left) and statistical analysis was made (Right). e Cell invasion of U2OS cells were inhibited after Herg1 knockdown, which was monitored by matrigel transwell assay. Representative images were displayed (Left) and statistical analysis was made (Right). **P < 0.01, ***P < 0.001.

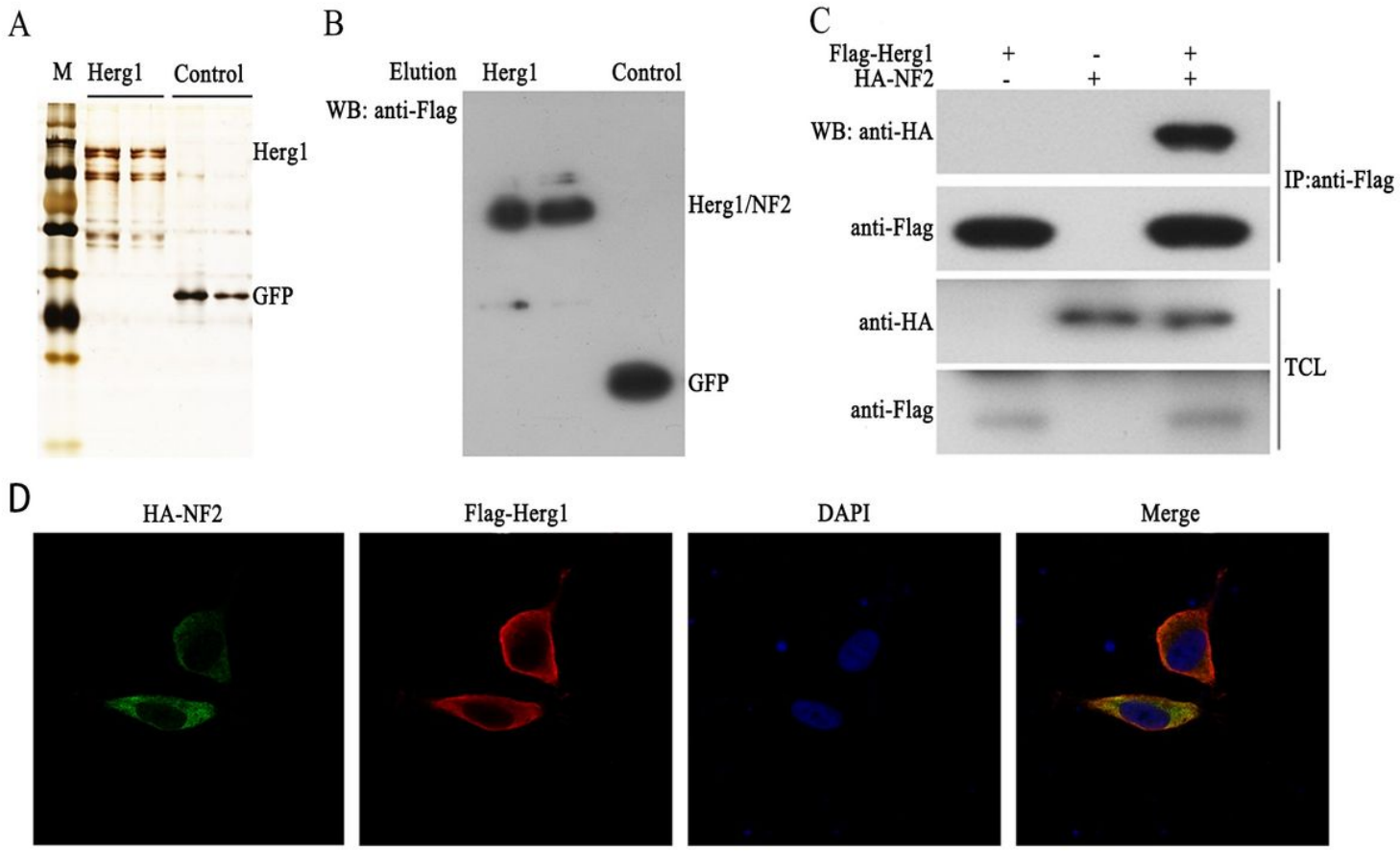

Figure 3

Herg1 co-localized and interacted with NF2. a Tandem affinity purification was performed to isolate Flag-Herg1 associated complex. b Western blotting was used to confirm the successful purification of Flag-Herg1. c Immunoprecipitation assay revealed that Flag-Herg1 interacted with HA-NF2. Flag-Herg1 and HA-NF2 were co-expressed in 293T cells, 48 h later, cells were lysed and subjected to immunoprecipitation assay by using anti-Flag antibody. d Immunofluorescent staining assay indicated that Herg1 co-localized with NF2 in the cell membrane. DAPI was used to stain the nuclei.

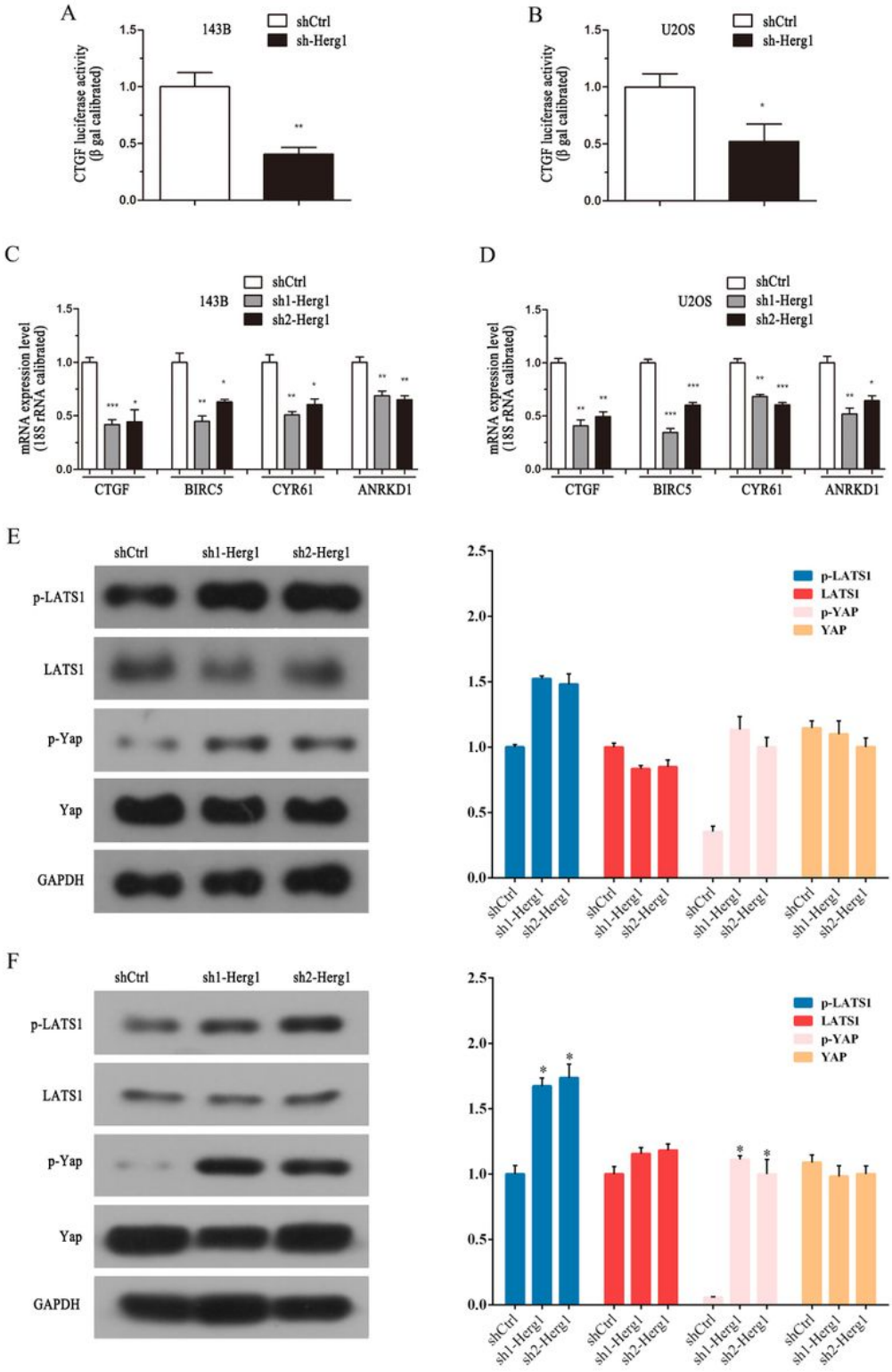

Figure 4

Knockdown of Herg1 turned on Hippo signaling pathway. a,b Knockdown of Herg1 decreased the CTGF luciferase activity in both 143B cells and U2OS cells. c,d Reduction of Herg1 down-regulated YAP downstream genes in both 143B cells and U2OS cells. Gene expression levels were normalized to ribosomal 18S RNA. e,f Knockdown of Herg1 elevated the phosphorylation levels of LATS1/2 and YAP in both 143B cells and U2OS cells. GAPDH was used as loading control. *P < 0.05, **P < 0.01, ***P < 0.001.

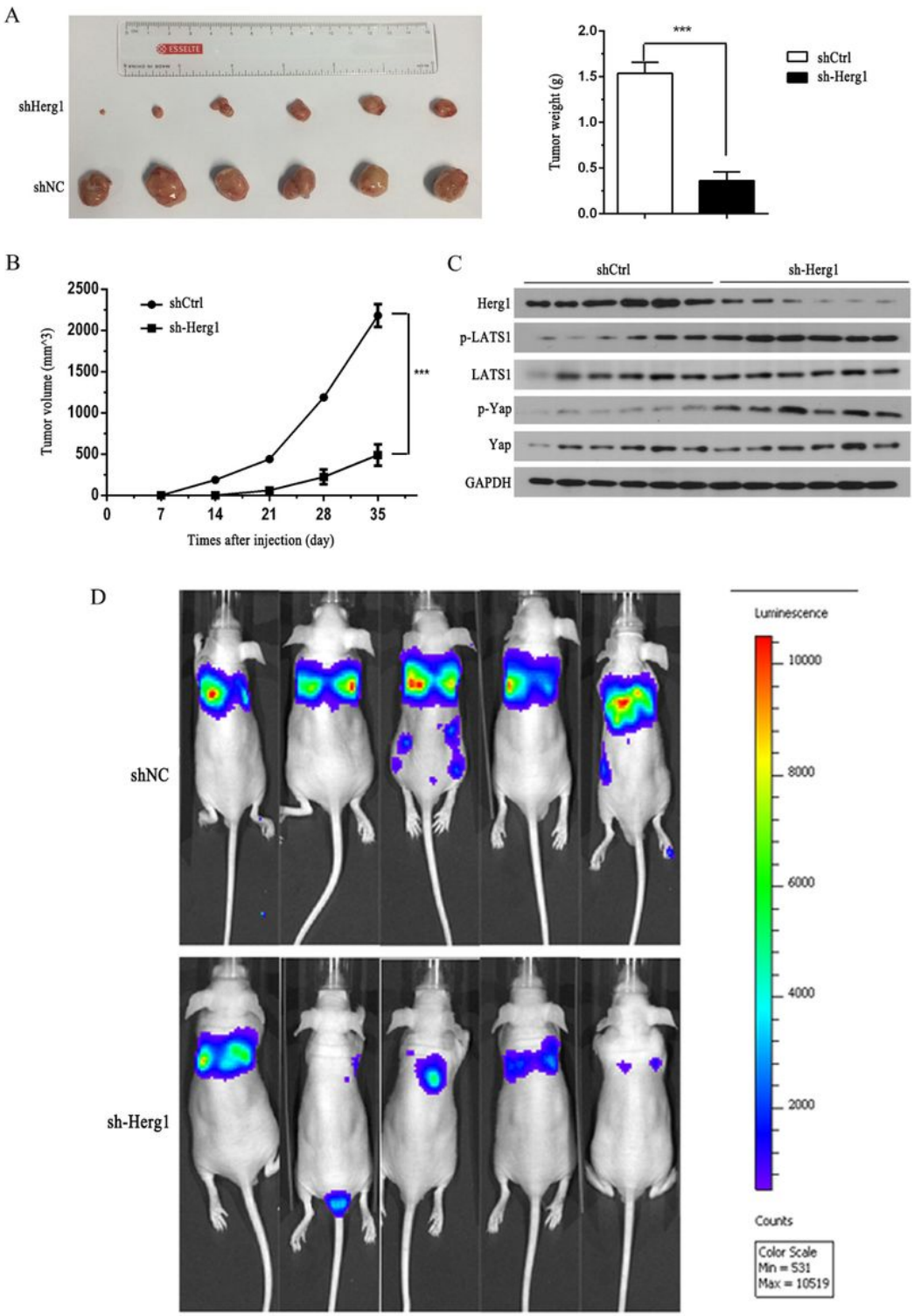

Figure 5

The functions of Herg1 were confirmed by in vivo mouse model. a shHerg1 mice had smaller tumor size compared to shNC cohorts. Xenografted tumors derived from shNC and shHerg1 mice (Left) and a statistical analysis was conducted (Right). b Tumor volume was weekly measured in shNC and shHerg1 mice by using this formula: ab2 × 0.5, where a was the length and b was the width of the tumor. c Western blotting result indicated that the phosphorylation levels of LATS1/2 and YAP were increased in

tumor samples derived from shHerg1 mice compared to the control cohorts. d shHerg1 mice had less metastatic foci in tail vein injection mouse model. ***P < 0.001.